УДК 551.465

© *В. М. Журбас, В. Т. Пака, М. Н. Голенко, А. О. Корж*
Институт океанологии им. П. П. Ширшова РАН, Москва
m.golenko@yahoo.com

ОЦЕНКА ТРАНСФОРМАЦИИ РАСПРОСТРАНЯЮЩЕЙСЯ НА ВОСТОК СОЛЕНОЙ ВОДЫ НА СЛУПСКОМ ПОРОГЕ БАЛТИЙСКОГО МОРЯ ПО ДАННЫМ МИКРОСТРУКТУРНЫХ ИЗМЕРЕНИЙ

Статья поступила в редакцию 14.09.2018, после доработки 29.01.2019

Измерения, выполненные в окрестности Слупского порога с помощью привязного свободно-падающего микроструктурного зонда, выявили наличие пятна с высоким уровнем скорости диссипации турбулентности непосредственно за порогом с восточной стороны в придонном слое, заполненном распространяющейся на восток соленой водой. Предложен метод, позволяющий количественно оценить роль топографического препятствия наподобие Слупского порога в перемешивании/трансформации затоковой воды по данным микроструктурных измерений. Для этого сначала по вертикальным профилям удельной скорости диссипации кинетической энергии турбулентности и потенциальной плотности рассчитывается скорость вовлечения воды пониженной солености из вышележащего слоя в придонный турбулентный слой соленой воды. Затем, полагая, что в придонном течении соленой воды критическое значение числа Фруда достигается непосредственно над порогом, оценивается расход течения. Наконец, из баланса между адвекцией и турбулентным вовлечением можно получить оценку изменения солености распространяющейся на восток соленой воды из-за интенсификации перемешивания в области порога. Получено, что локальное усиление турбулентного перемешивания в районе Слупского порога ответственно примерно за 5 % уменьшения солености затоковых вод на пути от Арконского бассейна до Готландской впадины.

Ключевые слова: Балтийское море, топографическое препятствие, микроструктурные измерения, скорость диссипации, вовлечение, гравитационное течение, эффективность перемешивания.

V. M. Zhurbas, V. T. Paka, M. N. Golenko, A. O. Korzh
Shirshov Institute of Oceanology of Russian Academy of Sciences, Moscow, Russia
m.golenko@yahoo.com

TRANSFORMATION OF EASTWARD SPREADING SALINE WATER AT THE SŁUPK SILL OF THE BALTIC SEA: AN ESTIMATE BASED ON MICROSTRUCTURE MEASUREMENTS

Received 14.09.2018, in final form 29.01.2019

Measurements performed by a loosely tethered free-falling microstructure profiler in the vicinity of the Słupsk Sill revealed a high turbulence dissipation spot immediately beyond the sill to the east in the near-bottom layer filled with eastward spreading saltwater. An approach is developed to quantitatively estimate the role of a topographic obstacle like the Słupsk Sill in mixing/transformation of inflow waters using data of microstructure measurements. To do this, first, based on vertical profiles of specific dissipation rate of kinetic energy of turbulence and potential density, the rate of entrainment of low salinity water from the overlying layer to the near-bottom turbulent saltwater layer is calculated. Then, assuming that in the near-bottom saltwater flow, the critical value of the Froude number is reached directly at the Sill, the flow volume rate is estimated. Finally, from the balance between advection and turbulent entrainment, the change in salinity of the eastward spreading saltwater due to intensification of mixing at the Sill can be evaluated. Using data of microstructure measurements available, the mixing hot spot at the Słupsk Sill was found to be responsible for approximately 5 percent of the inflow water salinity decrease en route from the Arkona Basin to the Gotland Deep.

Keywords: Baltic Sea, topographic obstacle, microstructure measurements, dissipation rate, entrainment, gravity flow, mixing efficiency.

Ссылка для цитирования: *Журбас В.М., Пака В.Т., Голенко М.Н., Корж А.О.* Оценка трансформации распространяющейся на восток соленой воды на Слупском пороге Балтийского моря по данным микроструктурных измерений // Фундаментальная и прикладная гидрофизика. 2019. Т. 12, № 2. С. 43–49.

For citation: *Zhurbas V.M., Paka V.T., Golenko M.N., Korzh A.O.* Transformation of eastward spreading saline water at the Słupk Sill of the Baltic Sea: an estimate based on microstructure measurements. *Fundamentalnaya i Prikladnaya Gidrofizika*. 2019, 12, 2, 43–49.

DOI: 10.7868/S2073667319020060

Introduction

The Słupsk Sill is a meridionally-aligned, saddle-shaped ridge between the Bornholm Deep in the west and the Słupsk Furrow in the east; the deepest point at the saddle is located at approximately 56 m depth (fig. 1). Dense, saline water of the North Sea origin has to overflow the sill to enter the Słupsk Furrow and further the deepest basins of the Baltic Proper. The passage of dense inflow water through a constriction like the Słupsk Sill is expected to be accompanied by enhanced mixing/turbulence and, probably, even by formation of the internal hydraulic jump.

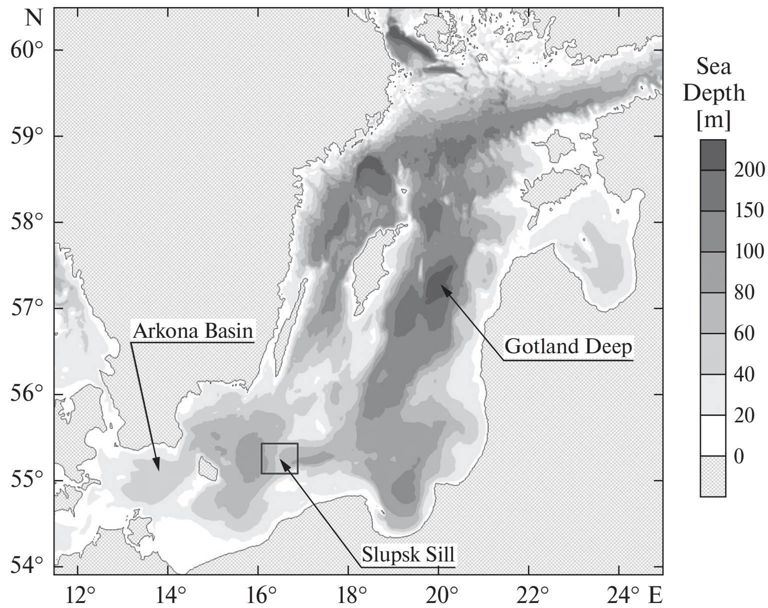

Fig. 1. Bathymetric map of the Baltic Sea. The Słupsk Sill area is marked by a rectangular (see a close-up of the area in fig. 2).

Рис. 1. Батиметрическая карта Балтийского моря.
Область Слупского порога отмечена прямоугольником (см. крупный план на рис. 2).

Based on measurements in a bottom gravity current in the Gulf of Cadis related to the Mediterranean Outflow, Nash et al. [1] pointed out the importance of small-scale features in the bottom topography. The flow appears to be hydraulically controlled at a small topographic constriction, with turbulence and internal waves varying together and increasing dramatically downstream of a choke point. Choke points in bottom gravity currents can feed turbulence that is orders of magnitude more intense than elsewhere; the turbulence mixing and entrainment can be focused in such hotspots.

Using microstructure measurements performed from an autonomous underwater vehicle in the Denmark Strait Overflow plume on the continental slope of Greenland 180 km downstream of the sill, Schaffer et al. [2] reported on a stationary high-dissipation event on the upstream side of a topographic elevation located in the gravity flow pathway.

The general purpose for this study is to quantitatively estimate the role of the Słupsk Sill in mixing/transformation of inflow waters based on direct measurements of turbulence/microstructure.

Instrumentation and Data

Microstructure measurements where performed using a loosely tethered free-falling microstructure profiler (MSP) "Baklan" [3] equipped with a rich set of sensors including fast velocity shear and fast temperature fluctuations, high resolution CTD, and 3D-accelerations. More specifically, the MSP was equipped with a PNS06 shear probe from ISW Wassermesstechnik, a fast thermistor (model FP07) from GE Thermometrics (a special design of the sensor by Idronaut S.r.l.), a 7-ring conductivity cell and high-precision temperature sensor from Idronaut S.r.l., a pressure sensor (model D-25) from PROMPRIBOR (www.prompribor.ru), a 3D-accelerometer (model ADXL203) from Analog Devices, Inc., and some auxiliary sensors reserved in the event of accidents.

The velocity shear probe signal was used to calculate the turbulent kinetic energy (TKE) dissipation ε by an expression of $\varepsilon = 7.5\nu\left\langle u_z'^2 \right\rangle$, where $\left\langle u_z'^2 \right\rangle$ is the variance of the vertical current shear fluctuations, $\nu = (1.79–1.31)10^{-6}$ m^{2}s^{-1} is the kinematic viscosity of water in the temperature range of 0–10 °C. The variance of the vertical current shear fluctuations in the 2–24 Hz frequency window was taken as the non-overlapping running mean of 500 counts of the vertical current shear fluctuation squared, which corresponds to vertical averaging over approximately 0.6 m.

In the 34th cruise of R/V AKADEMIK NIKOLAY STRAKHOV, two microstructure transects were performed in the Słupsk Sill area using MSP "Baklan" (see fig. 2). The first transect (July 2, 2017) consisting of 12 MSP casts, was directed across the sill (quasi-zonally), and the second one (July 4–5, 2017) consisting of 9 MSP casts was directed along the sill (quasi-meridionally) passing at a distance of approximately 8 km east (downstream) of the Sill.

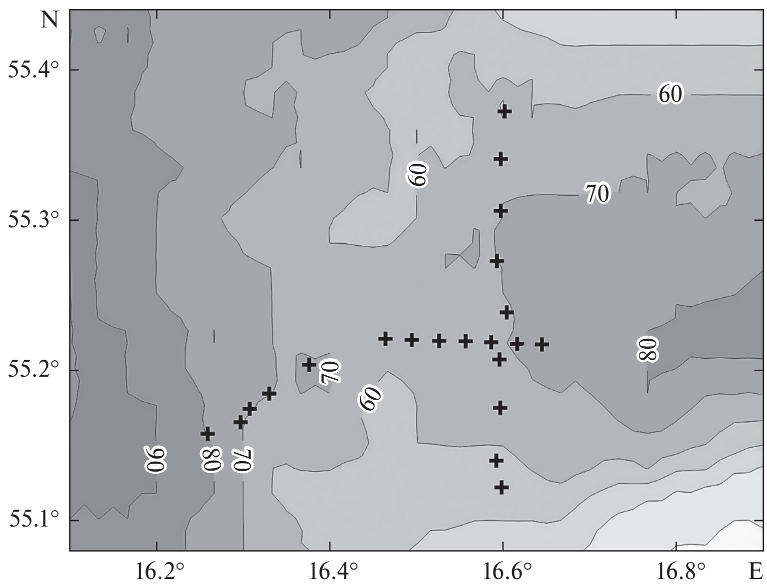

Fig. 2. Close-up bathymetric map of the Słupsk Sill area.
The black crosses depict the location of measurements by microstructure profiler "Baklan".
The cross-sill (quasi-zonal) and along-sill (quasi-meridional) transects were performed on July 2, 2017, and July 4–5, 2017, respectively.

Рис. 2. Крупный план области Слупского желоба.
Черными крестами отмечено положение измерений микроструктурным профилографом «Баклан».
Поперечный (квазизональный) и продольный (квазимеридиональный) порогу разрезы были выполнены 2 и 4–5 июля 2017 г. соответственно.

Approach

Our ultimate goal is a quantitative assessment of the effect of Słupsk Sill on mixing/transformation of inflow waters which can be characterized by so-called mixing efficiency of the sill, E_{sill} (to be defined below). The following approach is proposed to calculate E_{sill}.

Using vertical profiles of potential density $\rho(z)$ and TKE dissipation rate $\varepsilon(z)$, where z axis is directed upward and $z = 0$ is at the seabed, we calculate the bulk thickness, H, buoyancy jump, B, and entrainment rate, w_e, for the near-bottom gravity current, defined following [3, 4] as

$$BH = \int_0^\infty g\frac{\rho(z)-\rho(\infty)}{\rho_0}dz = \int_0^\infty g'(z)dz\,, \tag{1}$$

$$\frac{BH^2}{2} = \int_0^\infty g'zdz\,, \tag{2}$$

$$w_e = 2\int_0^\infty K_\rho N^2 dz / \int_0^\infty g'(z) dz, \tag{3}$$

where on practice ∞ means some level above the permanent pycnocline/halocline, N^2 is the buoyancy frequency squared, and K_ρ is the vertical turbulent diffusivity for density/buoyancy which can be parameterized following [5] as

$$K_\rho = \begin{cases} 0.2\nu\eta \;\; for \;\; 7 < \eta < 100 \\ 2\nu\eta^{1/2} \;\; for \;\; \eta > 100 \end{cases}, \tag{4}$$

where $\eta = \varepsilon/\nu N^2$ is the turbulence intensity parameter in a stratified media.

The moderate turbulence intensity regime ($7 < \varepsilon/\nu N^2 < 100$) corresponds to stationary turbulence [6], while the energetic regime ($\varepsilon/\nu N^2 > 100$) corresponds to growing turbulence [5]. In the original Osborn [6] formulation of stationary turbulence $K_\rho = 0.2\varepsilon / N^2$, and the entrainment rate (3) can be expressed as

$$w_e = 0.4\int_0^\infty \varepsilon(z) dz / \int_0^\infty g'(z) dz\,. \tag{5}$$

Performing calculations (1)—(5) for every microstructure cast on the transect, we arrive at the dependencies of $H(x)$, $B(x)$, and $w_e(x)$ versus the cross-sill distance x.

An increase of dense/saline water volume per unit of time and per unit of along-sill length due to entrainment from the above-lying layer can be calculated as

$$W = \int_{-\infty}^{\infty} w_e dx, \tag{6}$$

where $-\infty$ and ∞ mean some locations before (upstream) and behind (downstream) the sill, respectively, where the mixing effect of the sill becomes negligible (i.e., the turbulent spot related to the sill lies between these two locations).

If S_{bottom} and V are the inflow water salinity and the inflow volume rate per along-sill unit of length ($[V] = \mathrm{m^2/s}$) before the sill, due to entrainment caused by the sill, the inflow water salinity will be changed for

$$S_{mixture} = \frac{S_{bottom}V + S_{surface}W}{V + W}, \tag{7}$$

where $S_{surface}$ is the upper layer salinity. In view of (7), the mixing efficiency of the sill can be defined as

$$E_{sill} = \frac{S_{bottom} - S_{mixture}}{S_{bottom} - S_{surface}} = \frac{W}{V + W}\,. \tag{8}$$

By definition (see eq. (8)), the mixing efficiency of the sill is nil when the inflow water salinity downstream the sill has not changed relatively its value upstream the sill, and tends to 1 when, due to entrainment caused by the sill, the salinity jump between the surface and bottom layers vanishes. Note that in the case of inflow water in the Baltic Sea, the mixing efficiency does not reach 1 because salinity jump between surface and bottom layers does not vanish anywhere. The maximum value of mixing efficiency for inflows to the Baltic Proper, $E_{\max}$, can be estimated if we take in eq. (8) $S_{bottom} = 20$ PSU (typical value of the bottom layer salinity in the Arkona Basin), $S_{mixture} = 12$ PSU (typical value of the bottom layer salinity in the Gotland Deep), $S_{surface} = 7$ PSU (typical value of the surface layer salinity in the Baltic Proper):

$$E_{\max} = \frac{20 - 12}{20 - 7} = 0.62\,.$$

Taking into account the latter circumstance, it is reasonable to re-define the mixing efficiency of the sill (8) as

$$E_{sill} = \frac{W}{V + W}\frac{1}{E_{\max}}\,. \tag{9}$$

The main problem with the approach (1)—(9) lies in V which is unknown since we have no current velocity measurements in the near bottom, high salinity layer because the down-looking from sea surface ADCP profilers display a “dead zone” of approximately 5—8 m thick adjacent the seabed. We can present the volume rate of inflow water as $V = H_{sill}U_{sill}$, where H_{sill} and U_{sill} are the bulk thickness and velocity of near-bottom inflow layer at the sill, respectively, and, in view of the lack of velocity measurements, apply some physical principle to access U_{sill}. Namely, we can suppose that the Froude number of the gravity flow, $Fr(x) = U(x) / \sqrt{B(x)H(x)}$, where $U(x)$ is the bulk velocity of gravity flow, reaches the critical value of 1 just above the sill: $U_{sill} = \sqrt{B_{sill}H_{sill}}$, where B_{sill} is the bulk value of buoyancy jump at the sill. Therefore, we can estimate the inflow volume rate at the sill as $V = B_{sill}^{1/2} H_{sill}^{3/2}$ and rewrite (9) as follows

$$E_{sill} = \frac{W}{V+W}\frac{1}{E_{\max}} = \frac{\int_{-\infty}^{\infty} w_e dx}{B_{sill}^{1/2} H_{sill}^{3/2} + \int_{-\infty}^{\infty} w_e dx}\frac{1}{E_{\max}}. \quad (10)$$

Results

Oceanographic parameters such as temperature t, salinity S, potential density anomaly σ_θ, squared buoyancy frequency N^2, and TKE dissipation rate ε versus distance [km] and depth [m] at the cross-sill and along-sill transects are presented in fig. 3, left- and right-hand panels, respectively; see insert.

The most prominent feature of the cross-sill transect is well-pronounced, highly turbulent spot in the bottom layer immediately behind the shallowest point of the transect (i.e. behind the sill) to the east (downstream relatively to inflow water propagation). (Note that similar observations of a highly turbulent spot behind the Słupsk Sill was recently reported by Mohrholz and Heene [7] interpreting it in terms of internal hydraulic jump.) Other interesting feature is that the near-bottom turbulent spot is well-mixed vertically and bounded from above by a thin interface layer with enhanced buoyancy frequency (relative to a thicker interface with decreased buoyancy frequency upstream), which can be treated as a signature of enhanced vertical mixing and entrainment.

On the meridional, along-sill transect located downstream the sill, one can observe a salt/dense water pool to the south of the deepest point (on the southern slope) corresponding to an eastward gravity flow in view of geostrophic balance. The bottom gravity flow is highly turbulent with dissipation rate ε up to $5 \cdot 10^{-6}$ W/kg. Note that the maximum density location is shifted to the northern tip of the dense water pool in accordance to the northern direction of the Ekman transport beneath the eastward bottom gravity current [8]. Also it is seen from comparison of fig. 3, the left and right panels, that typical value of ε observed in the along-sill transect of the gravity current was 3—4 times higher than in the cross-sill transect. Keeping in mind that the along-sill transect was performed 2 days after the cross-sill transect, the difference in the typical ε estimates can be attributed to temporal variability of the dissipation level in gravity current.

In addition to vertical transects of dissipation rate ε (fig. 3, the bottom panels), it might be interesting to see the same for the vertical eddy diffusivity K_ρ calculated by means of (4). Variability of K_ρ versus the cross-sill distance and depth is mostly similar to that of ε (fig. 4 and fig. 3, the left bottom panel; see insert). The highest values of K_ρ of the order of 0.01 m^2/s are observed in the surface layer which is directly affected by atmospheric forcing, while in the bottom layer K_ρ increases to $1 \cdot 10^{-4}$—$1 \cdot 10^{-3}$ m^2/s relatively to low values of the order of $1 \cdot 10^{-6}$ in the water column interior.

The $H(x)$, $B(x)$, and $w_e(x)$ versus the cross-sill distance x calculated from equations (1)—(5) for the cross-sill transect are presented in table.

Using data presented in table and performing integration in eq. (6), we get $W = 1.38 \cdot 10^{-2}$ and $2.04 \cdot 10^{-2}$ m^2/s for the increase of dense/saline water volume due to entrainment by the sill per unit of time and sill’ width (in accordance to eqs. (3) and (5), respectively).

Since in the along-sill transect, the typical value of ε in gravity flow was 3—4 times higher than in the cross-sill transect, the upper estimate of W from the microstructure measurements available is supposed to be as high as $W = 4 \cdot 2.04 \cdot 10^{-2} \approx 0.08$ m^2/s. Then, taking $H_{sill} = 5.54$ m and $B_{sill} = 3.51\ 10^{-2}$ m/s^2 in accordance to table, we get $V = B_{sill}^{1/2} H_{sill}^{3/2} = 2.4$ m^2/s for the volume rate of the dense/saline overflow per unite of sill’ width. Therefore, in accordance to microstructure measurements available, turbulent entrainment

Table

Parameters H, B, w_e, and the sea depth versus the distance x for the cross-sill transect.
Параметры H, B, w_e, и глубина моря на расстоянии x от начала разреза через Слупский порог

Cast#	Lon [°]	Lat [°]	H_{sea} [m]	x [km]	H [m]	B [10^{-2}m/s^2]	w_e (3) [10^{-7}m/s]	w_e (3′) [10^{-7}m/s]
5	16.2589	55.1578	75.4	0	21.93	5.89	1.94	5.69
6	16.2969	55.1656	69.6	2.56	17.68	4.98	1.27	1.27
7	16.3076	55.1745	68.7	3.77	17.3	4.84	2.44	2.62
8	16.3304	55.1847	66.3	5.61	15.66	4.65	2.77	3.23
10	16.3761	55.2039	63.1	9.20	13.99	4.42	2.81	3.35
14	16.4641	55.2212	55.1	15.55	6.82	4.01	3.2	4.47
15	16.4949	55.2202	54.5	17.50	5.54	3.51	13.7	14.4
16	16.5261	55.2197	57.0	19.48	5.55	3.89	17.5	26.4
17	16.5569	55.2194	58.9	21.43	5.58	4.23	10.2	24.3
18	16.5863	55.2187	61.1	23.30	6.44	4.34	3.71	4.76
19	16.6161	55.2178	65.5	25.19	10.41	4.49	1.5	2.94
20	16.6447	55.2174	68.2	27.00	11.78	4.32	4.4	6.04

by the Słupsk Sill can cause an increase of the volume rate of the dense/saline water overflow (and related decrease of the density/salinity jump) up to 3.3%. Finally substituting the above values of W, V and $E_{\max}$ to eq. (10), we assess the mixing efficiency of the Słupsk Sill such as $E_{sill} = 0.052$. The latter estimate says that the Słupsk Sill is responsible for approximately 5 percent of the inflow water salinity decrease on route from the Arkona Basin to the Gotland Deep.

Discussion and Conclusions

In this paper, an approach to estimate mixing efficiency of a topography constriction for near-bottom gravity flows is proposed based on direct (microstructure) measurements of the TKE dissipation rate. The approach is applied to data of microstructure profiling in the vicinity of the Słupsk Sill when a well-pronounced, highly turbulent spot was recorded in the bottom layer immediately behind the shallowest point of the sill to the east (downstream relatively to inflow water propagation). In accordance to microstructure measurements available, the Słupsk Sill is estimated to be responsible for approximately 5 percent of the inflow water salinity decrease on route from the Arkona Basin to the Gotland Deep.

There are several topography constrictions along the inflow pathway in the Baltic Sea such as the Bornholm Strait, the Słupsk Sill, the Słupsk Furrow outlet, and an elevation at the eastern slope of the Hoburg Channel approximately on the beam of Klaipeda (see fig. 1), where simulations [9] displayed an enhancement of the bottom friction velocity, and each of them can contribute to transformation of inflow water due to enhanced turbulence. If one suggests that each of four abovementioned constrictions has mixing efficiency of the same value, the cumulative mixing efficiency of the topography constrictions can reach 20%. The remaining 80% of the bottom salinity decrease en route from the Arkona Basin to the Gotland Deep are probably caused by turbulent mixing produced by bottom friction in the gravity current of inflow water away from the topographic constrictions, as well as by near-inertial internal waves [10]. However, we do not exclude that the above approach underestimate to some extent the role of the Słupsk Sill in transformation/mixing of the inflow waters, because in view of the lack of current velocity measurements in the near-bottom layer we applied the assumption of critical regime of gravity flow at the sill.

Collection and pre-processing of the field data were carried out in the framework of the state assignment of IO RAS (theme N0149-2019-0013*), the data analysis and interpretation — in the framework of the state assignment of IO RAS (theme* N0149-2019-0003*). Development and realization of the approach to estimate effect of the sill on water mass transformation was supported by the Russian Foundation for Basic Research (Grant* N18-05-80031*).*

Литература

1. *Nash J.D.*, *Peters H.*, *Kelly S.M.*, *Pelegrí J.L.*, *Emelianov M.*, *Gasser, M.* Turbulence and high-frequency variability in a deep gravity current outflow // J. Geophys. Let. 2012. 39. L18611. P. 1–6.
2. *Schaffer J.*, *Kanzow T.*, *Jochumsen K.*, *Lackschewitz K.*, *Tippenhauer S.*, *Zhurbas V.M.*, *Quadfasel D.* Enhanced turbulence driven by mesoscale motions and flow topography interaction in the Denmark Strait Overflow plume // J. Geophys. Res. Oceans. 2016. 121(10). P. 1–23.
3. *Paka V.*, *Zhurbas V.*, *Rudels B.*, *Quadfasel D.*, *Korzh A.*, *Delisi D.* Microstructure measurements and estimates of entrainment in the Denmark Strait overflow plume // Ocean Science. 2013. 9. P. 1003–1014.
4. *Arneborg L.*, *Fiekas V.*, *Umlauf L.*, *Burchard H.* Gravity Current Dynamics and Entrainment – A Process Study Based on Observations in the Arkona Basin // J. Phys. Oceanogr. 2007. 37. P. 2094–2113.
5. *Shih L.H.*, *Koseff J.R.*, *Ivey G.N.*, *Ferziger J.H.* Parameterization of turbulent fluxes and scales using homogeneous sheared stably stratified turbulence simulations // J. Fluid Mech. 2005. 525. P. 193–214.
6. *Osborn T.* Estimates of the local rate of vertical diffusion from dissipation measurements // J. Phys. Oceanogr. 1980. 10. P. 83–89.
7. *Mohrholz V.*, *Heene T.* The Słupsk Sill overflow – mixing hot spot of the eastward spreading saline water // 2nd Baltic Earth Conference, Helsingør, Denmark, 11 to 15 June 2018. Conference Proceedings. P. 28–29. URL: https://www.baltic-earth.eu /helsingor2018/ material/2ndBalticEarthConferenceProceedings_IBESP%20No13.pdf (дата обращения: 01.09.2018).
8. *Paka V.T.*, *Zhurbas V.M.*, *Golenko N.N.*, *Stefantsev L.A.* Effect of the Ekman transport on the overflow of saline waters through the Słupsk Furrow in the Baltic Sea // Izvestiya – Atmospheric and Ocean Physics. 1998. 34(5). P. 641–648.
9. *Zhurbas V.*, *Väli G.*, *Golenko M.*, *Paka V.* Variability of bottom friction velocity along the inflow water pathway in the Baltic Sea // J. Mar. Syst. 2018. 184. P. 50–58.
10. *van der Lee E.M.*, *Umlauf L.* Internal wave mixing in the Baltic Sea: Near-inertial waves in the absence of tides // J. Geophys. Res. 2011. 116. C10016. P. 1–16.

References

1. *Nash J.D.*, *Peters H.*, *Kelly S.M.*, *Pelegrí J.L.*, *Emelianov M.*, *Gasser, M.* Turbulence and high-frequency variability in a deep gravity current outflow. *J. Geophys. Let*. 2012, 39, L18611, 1–6.
2. *Schaffer J.*, *Kanzow T.*, *Jochumsen K.*, *Lackschewitz K.*, *Tippenhauer S.*, *Zhurbas V.M.*, *Quadfasel D.* Enhanced turbulence driven by mesoscale motions and flow topography interaction in the Denmark Strait Overflow plume. *J. Geophys. Res. Oceans*. 2016, 121(10), 1–23.
3. *Paka V.*, *Zhurbas V.*, *Rudels B.*, *Quadfasel D.*, *Korzh A.*, *Delisi D.* Microstructure measurements and estimates of entrainment in the Denmark Strait overflow plume. *Ocean Science*. 2013, 9, 1003–1014.
4. *Arneborg L.*, *Fiekas V.*, *Umlauf L.*, *Burchard H.* Gravity Current Dynamics and Entrainment – A Process Study Based on Observations in the Arkona Basin. *J. Phys. Oceanogr*. 2007, 37, 2094–2113.
5. *Shih L.H.*, *Koseff J.R.*, *Ivey G.N.*, *Ferziger J.H.* Parameterization of turbulent fluxes and scales using homogeneous sheared stably stratified turbulence simulations. *J. Fluid Mech*. 2005, 525, 193–214.
6. *Osborn T.* Estimates of the local rate of vertical diffusion from dissipation measurements. *J. Phys. Oceanogr*. 1980, 10, 83–89.
7. *Mohrholz V.*, *Heene T.* The Słupsk Sill overflow – mixing hot spot of the eastward spreading saline water. *2nd Baltic Earth Conference*, *Helsingør*, *Denmark*, 11 to 15 June 2018. *Conference Proceedings*. P. 28–29. URL: https://www.baltic-earth.eu / helsingor2018/ material/2ndBalticEarthConferenceProceedings_IBESP%20No13.pdf (date of access: 01.09.2018).
8. *Paka V.T.*, *Zhurbas V.M.*, *Golenko N.N.*, *Stefantsev L.A.* Effect of the Ekman transport on the overflow of saline waters through the Słupsk Furrow in the Baltic Sea. *Izvestiya – Atmospheric and Ocean Physics*. 1998, 34(5), 641–648.
9. *Zhurbas V.*, *Väli G.*, *Golenko M.*, *Paka V.* Variability of bottom friction velocity along the inflow water pathway in the Baltic Sea. *J. Mar. Syst*. 2018, 184, 50–58.
10. *van der Lee E.M.*, *Umlauf L.* Internal wave mixing in the Baltic Sea: Near-inertial waves in the absence of tides. *J. Geophys. Res*. 2011, 116, C10016, 1–16.

К статье *Журбас В. М.* и др. Оценка трансформации...

Zhurbas V. M. et al. Transformation of eastward...

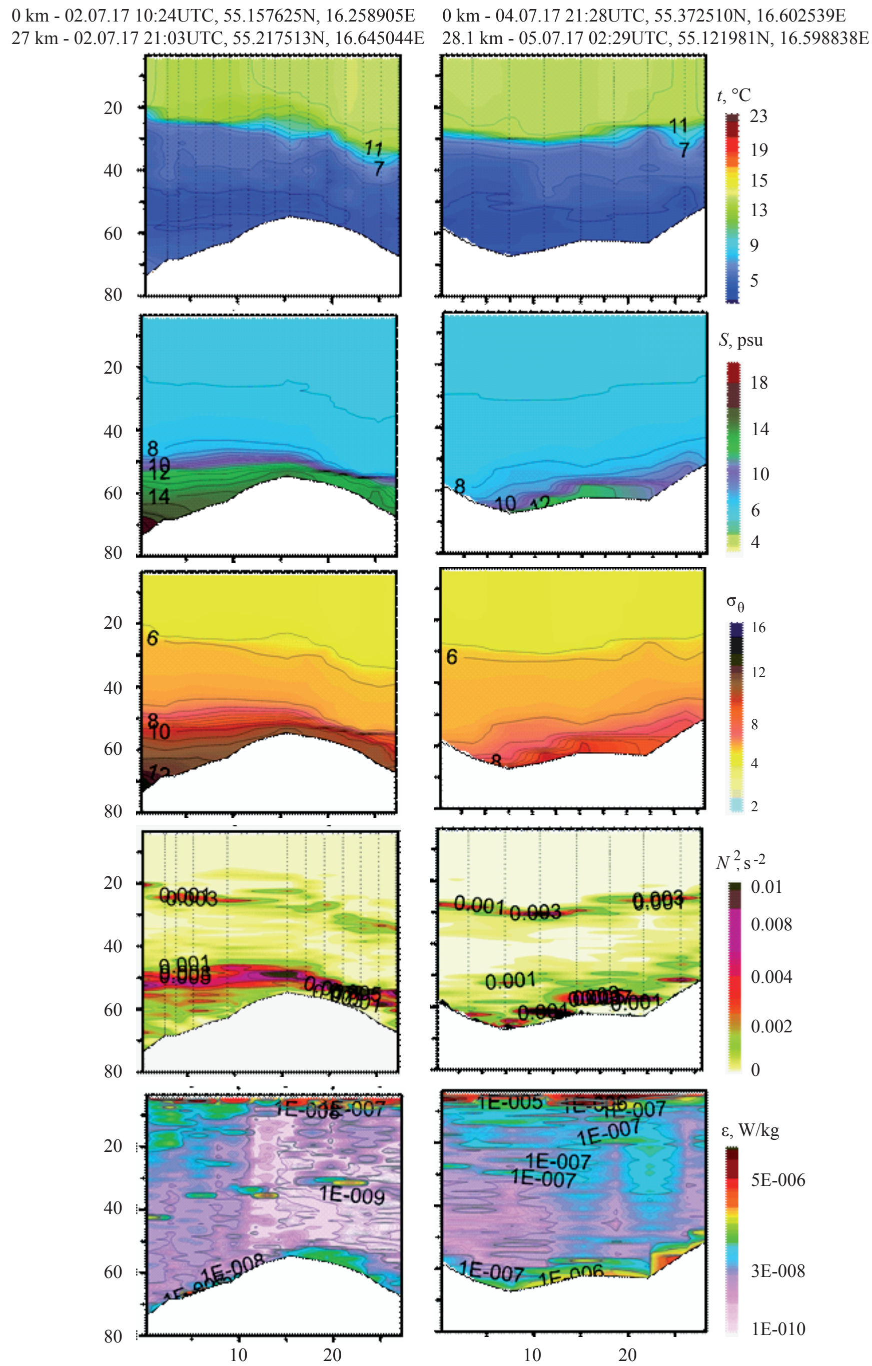

Fig. 3. Temperature t, salinity S, potential density anomaly σ_θ, squared buoyancy frequency N^2, and dissipation rate of turbulence kinetic energy ε versus distance [km] and depth [m] for the transects across (left) and along (right) the Słupsk Sill. Note that the distance axis is directed to the east for the left-hand panels and to the south for the right-hand panels.

Рис. 3. Температура t, соленость S, аномалия потенциальной плотности σ_θ, квадрат частоты плавучести N^2 и удельная скорость диссипации кинетической энергии турбулентности ε в координатах расстояние (км) и глубина (м) на разрезах поперек (слева) и вдоль (справа) Слупского порога. Заметим, что ось расстояния направлена на восток на левой панели и на юг на правой панели.

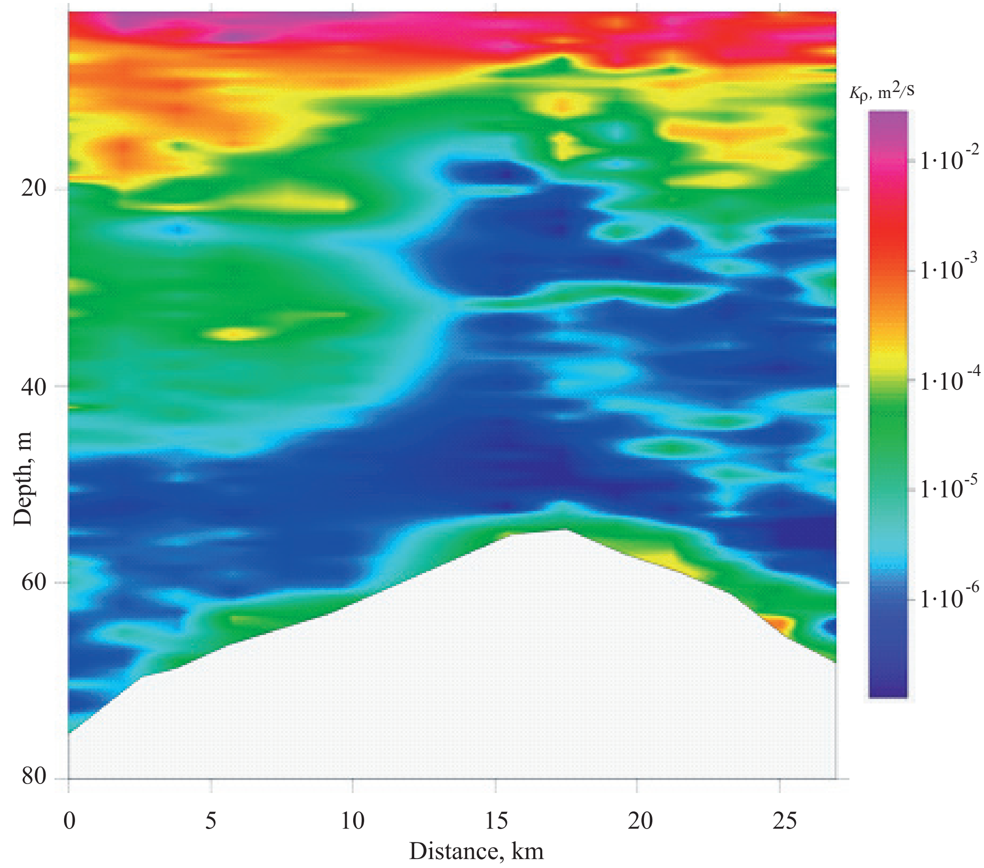

Fig. 4. Vertical eddy diffusivity K_ρ versus distance and depth for the transect across the Słupsk Sill.

Рис. 4. Коэффициент вертикальной турбулентной диффузии K_ρ в координатах расстояние и глубина на разрезе поперек Слупского порога.